



HAL
open science

A new component mode synthesis for dynamic mixed thin plate finite element models

Pierre Garambois, Sébastien Besset, Louis Jézéquel

► **To cite this version:**

Pierre Garambois, Sébastien Besset, Louis Jézéquel. A new component mode synthesis for dynamic mixed thin plate finite element models. *Archive of Applied Mechanics*, 2015, 10.1007/s00419-015-1072-x . hal-01266847

HAL Id: hal-01266847

<https://hal.science/hal-01266847>

Submitted on 7 Feb 2016

HAL is a multi-disciplinary open access archive for the deposit and dissemination of scientific research documents, whether they are published or not. The documents may come from teaching and research institutions in France or abroad, or from public or private research centers.

L'archive ouverte pluridisciplinaire **HAL**, est destinée au dépôt et à la diffusion de documents scientifiques de niveau recherche, publiés ou non, émanant des établissements d'enseignement et de recherche français ou étrangers, des laboratoires publics ou privés.

A new component mode synthesis for dynamic mixed thin plate finite element models

Pierre Garambois · Sébastien Besset ·
Louis Jézéquel

Received: date / Accepted: date

Abstract This paper presents a methodology for the reduction of Dynamic Mixed Finite Element Models (DM-FEMs) based on the use of a sub-structuring primal methods adapted to such models. We implement a DM-FEM for Kirchhoff-Love (KL) thin plates using the Hellinger-Reissner (HR) variational mixed formulation adapted to dynamic, and give a quick insight of its convergence. This model uses both displacement and generalized stress fields within the plate, obtained as a primary result, but the numerical size of the model is bigger than with a primal displacement model. Thus we choose to offset this complication by reducing the model with a totally new sub-structuring reduction method, especially adapted to DM-FEMs. The aim of our method is to adapt sub-structuring reduction methods commonly used for primal displacement FEM only (such as Craig & Bampton method) and split the reduction of the two fields. With these displacement methods, the whole structure is splitted into few smaller ones, and each of them is condensed with eigenmodes of the sub-structure and static connections between them. The principle of our method is to build, for each sub-structure, a reduced basis for the displacements according to the existing method, and a projection of the primal basis for the stresses. A new reduced basis for the whole mixed model is then built up exclusively with modes taken from the primal model. That method reduces significantly the number of degrees of freedom (DOF), and keeps the properties and advantages of the mixed formulation.

Keywords Component Mode Synthesis (CMS) · mixed finite element · reduction · sub-structuring · vibrations · plates

1 INTRODUCTION

Engineering plate problems are often described by partial differential equations. Thus, approximate numerical methods to solve them have been widely used in

P. Garambois · S. Besset · L. Jézéquel
LTDS, Ecole Centrale de Lyon · 36 av. Guy de Collongues, 69130 Ecully
E-mail: pierre.garambois@ec-lyon.fr

S. Besset
E-mail: sebastien.besset@ec-lyon.fr

L. Jézéquel
E-mail: louis.jezequel@ec-lyon.fr

many disciplines, especially for buckling, bending and vibrations analysis of isotropic plates and composite structures. We can make the distinction between meshed methods and meshless methods. In the group of meshed methods, Finite Element Models (FEMs), Finite Differences Methods (FDM) and Differential Quadrature (DQ) are widely used. DQ [52,75] and Harmonic DQ (HDQ) methods [25] permit to approximate partial derivatives by weighted linear summation of specific values and thus solve initial and boundary value. Compared to FEM and FDM, it only needs to use a few grid points to get a higher resolution and less computational cost. In spite of this, FEM are still mostly used in industry because they are simply implementable and they give an efficient representation of big complex systems and loads, especially for non-linear behavior. In the field of meshless method, some have shown interesting results, such as Discrete Singular Convolution (DSC) [26,27] that discretizes the spatial derivatives and transform them into eigenvalue problem, the wavelet collocation methods [36] or the radial basis function methods [80]. In our case, the idea is to work on FEM because it still represents the most popular way to treat efficiently engineering problems in industry and there is still a lot to learn and improve in this field.

Most of the FEM used in industry for structural mechanical problems are based on a dynamic primal displacement formulation. This displacement approach in FEMs have largely been developed [81,28,1]. They are fast and efficient, but they need an extra calculation and integration to get the strains and the stresses. They may also show some computational difficulties when it comes to plate and shell theories representation. Other numerical solutions providing stresses as primary results and solving computational problems have always been a major concern in mechanical engineering. A force approach based on direct calculation of the stresses was pioneered in FEMs by Fraejijs de Veubeke [37,38] and then by Pian and Tong [60,73] were made. Another method, called "mixed formulation" or "Reissner Mixed Variational Theorem" (RMVT), is based on the Hellinger-Reissner (HR) variational functional and defines a new "mixed" Lagrangian using both displacement and stress fields in the same functional, whereas the stresses depend on displacement in a displacement formulation. It was imagine for the first time by Hellinger [42] and Prange [61], and later by Reissner [65,66,67] and Arnold [3,2]. Generalized variational principles are well explained in Washizu's book [77]. Over the past four decades, many mixed FEM have been implemented, originally with Herrmann [45,46] who implemented one of the first mixed plate FEM using this RMVT and taking shear phenomena into consideration, quickly followed by other researchers [15,23]. Over the last forty years, many mixed FEMs have been implemented for different theory such as 3D problems [59], elastic arches problems [41], Timoshenko's beams [71,72] and particularly for plates [71,72,32,31,68]. Wriggers' book [78] provides a wide range of application for mixed FEM. Stability [6,13] and convergence [4] depending on the space fields of such elements have also been widely discussed. FEMs implemented with RMVT may present two main advantages in general: a direct access to stress parameters without post-processing, and a better representation of certain two-dimensional theories such as thick plates.

As far as stress access is concerned, researches have been made in order to easily get to the strain and stress fields, starting from a displacement approach. The classical methods used by most of the software in industry is the Gauss Points Method, that approximates an integral of a function with a weighted sum of function values at specified points within the elements. Other stresses and strains recovery methods were recently developed by Tornabene and Fantuzzi in the field of arbitrarily shaped laminated plates [33,34,35,74]. They implemented a Strong Formulation FEM (SFEM) using the strong formulation of the differential system

at the master element level. These models combined the generality of FEM and the accuracy of Spectral Methods (SM). Their method is based on the use of Generalized Differential Quadrature (GDQ) which approximates some derivatives (of both strains/stresses). That method permits a good representation of both in-plane and out-of-plane stresses/strains, for both static [33,34,35,74] and dynamic [35] analysis. Another method to access strain/stress values within an element formulates the initial problem in a "mixed" way, in function of both displacement and stress parameters, using the RMVT.

The use of such a mixed theorem has been mainly popularized in the context of plate and shell structures analysis, when three-dimensional descriptions try to be obtained with two-dimensional models, because it provides some computational advantages regarding such theory. Indeed, structural plates have a multitude of applications in industries and has received the attention of many researchers. The Kirchhoff-Love (KL) thin plate theory, originally developed by Love [54], is simply implementable and takes into consideration bending and twisting moments but doesn't deal with shearing phenomena which appear to be essential with moderately thick and thick plates. Thus, the Reissner-Mindlin (RM) theory for thick plates naturally appeared [64,56]. Nevertheless, thick RM plate may suffer from "shear-locking" problems and their representation can be tricky. In order to avoid computational problems, solutions have been imagined over the years [47,7,8,51,70,12,50,57,79] and among them, mixed type methods have shown very successful results [68,31,32,71,72,5], and thus justify its wide use in addition to the stress access previously mentioned. Other type of representations for plate and shell have been introduced by Henshell for hybrid/mixed element using specific continuity conditions [43] and rectangular elements with a high number of nodes [44]. In our case, although the mixed theory can solve locking problems for thick plate with certain continuity conditions, we want to focus more on the easy access to the stress parameters and especially show the benefit of the reduction method. This is the reason why we build a thin plate finite element model that is rather simple in terms of continuity conditions and do not focus on the thick plates issues. Mixed FEM are also widely used in the field of laminated multilayered plate structure and piezoelectric multilayered structures because of the increasing use of composites in thick and thin structures in industry. Indeed, the evaluation of normal stress and transverse shear is crucial in composites, and Equivalent Single Layer (ESL) models using displacement approach have been imagined to represent multilayered structure. They present the advantage of a number of unknowns independent from the number of layers but it does not fulfill some continuity requirements and post-processing can show inaccurate results in the case of thick plates. Furthermore, High-order Shear Deformation Theory (HSDT [53]), developed by Cho and Parmerter [24], although including some continuity requirements, experiences difficulties with analyzing problems in which out-of-plane stress play an important role. Another model called LayerWise Model (LWMs) considers each layer as a single plate [69,62], and gives acceptable results but does not fulfill interlaminar continuity, and have a much bigger size. In this context, mixed models using RMVT have retained attention in this field as they a priori and completely verify C_z^0 -requirement, and give a good description of transverse stresses. In this way, mixed layerwise theory to calculate in-plane and out-of-plane stresses/strains for thick multilayered orthotropic laminated plates have been implemented by Carrera for static analysis [17,21,22], thermo-static stress analysis [18] and well reviewed in [19] for both ESL and LWM theories. FEMs deep development of such theory is also available in [21,22]. The comparison between the Principle of Virtual Displacements (PVD) used in primal displacement approached and RMVT-based mixed model [17,19,21,22] gives a clear advantage to the mixed formulation, in

terms of interlaminar displacement and stress continuity as well as a good description of stresses within the structure.

As far as piezoelectric adaptive plate is concerned, mixed formulation has also proved to be efficient. Although primal models exist [9], and some of them fulfill interlaminar continuity implementation [16], the use of mixed Layerwise theory for piezoelectric adaptive structure has also proved to be of a high interest in static and modal analysis [39,40], thermodynamic analysis [10]. Carrera and Boscolo's article [20] shows an extension to electro-mechanical piezoelectric plate problems of a previously cited article by Carrera [21,22] on both primal and mixed FEM for multilayered plate elements using both ESL and LWM theories. This article puts forward another use and interest of mixed model in structural mechanical and FEMs analysis.

Although showing some benefits for the reasons previously defined, an obvious inconvenience of the mixed formulation, is the numerical size of the problems, due to the addition of stress fields parameters (generalized stress in a plate case) to the displacement field parameters of a regular primal method. Many reserachers even consider that any advantage of the mixed FEM is outweighed by the problem size. That is the reason why our work focus on finding a numerical solution in order to reduce such models, meanwhile keeping the mixed benefits.

In this paper, the mixed FEM we choose as a test model for the reduction methods, is voluntarily simple as it is not the main point of the study. It is a Dynamic Mixed Finite Element Model (DM-FEM) implemented with RMVT for thin KL plate elements, in which displacements and generalized stresses are parameters of the problem. Most of the time, the cited examples of mixed FEM deals with static analysis. It is more rarely used for free vibrations [58], and when it is, it often condenses the problems with condensed (or equivalent) stiffness on the displacement and then make the calculation only on this field. The idea of our sub-structuring method is to reduce the full model in order to keep stresses as a primary result. Indeed, the mixed model used in this paper is a Dynamic Mixed FEM (DM-FEM) that takes into consideration the kinetic energy in the mixed formulation and keep both fields in the model. Besides implementing the whole FEM on Matlab, we implemented a method of assembling to build highly meshed structures.

Many sub-structuring reduction methods called Component Mode Synthesis (CMS) methods exist in order as to reduce primal displacement FEM such as: "fixed interface mode" method (Craig & Bampton method [30,29,14]), "free interface mode" method (Mac Neal method [55]) and "boundary mode" method (see Brizard [14] and Tran [76]). The principle of these methods is to split the global structure into a few sub-structures, to describe each of them with a truncated basis made of their proper eigenmodes (the type of eigenmodes depending on the method) before re-assembling them. Some of those methods have also been associated to build up a Double Modal Synthesis (DMS) or Double Component Mode Synthesis (Double CMS, see Jezequel [48,49] and Besset [11]) that both condenses the sub-structures and the junction between them with "boundary modes". In the case of a mixed FEM, the constitutive matrices are singular and it is impossible to compute the modes of the structure. In this way we cannot use these methods, as originally formulated. Our work is to adapt them in order to build up a new reduced basis for each mixed sub-structure. The main idea is, for each sub-structure, to separate the condensation of each of the two fields, using the primal Craig & Bampton method [30,29,14] for the condensation of the displacements and a projection of this method on the stresses for the latter. Once the reduction

of the two fields is made, we build up a whole mixed basis for each sub-structure and we assemble them through the displacement parameters. It is to be noticed that the method we implement here remains identical for any displacement-stress mixed FEM using any mechanical theory (plate, beam, 3D, arches...).

First of all, the article presents the HR mixed variational dynamic formulation, its application to FE for KL theory in the case of thin plates, and quickly discuss the convergence of the two mixed model. In the next part, we present a CMS sub-structuring methods based on "fixed interface modes" and its application to the DM-FEM. In the end, we deal with the convergence of the reduction method implemented in function of the truncation on a simple example and present the main results.

2 MIXED VARIATIONAL FORMULATION AND MIXED FINITE ELEMENT MODEL BASED ON THIN PLATE THEORIES

In this section, we use Einstein summation convention to manipulate physical equations with coordinates. The Cartesian coordinates system leads us to a subscript i that corresponds to x, y, z . The following examples illustrate the meaning of this convention in our case:

$$\mathbf{b}_i \mathbf{u}_i = \{b_x \ b_y \ b_z\} \begin{Bmatrix} u_x \\ u_y \\ u_z \end{Bmatrix} \quad (1)$$

$$\boldsymbol{\sigma}_{ij} \mathbf{e}_{ij} = \{\epsilon_{xx} \ \epsilon_{yy} \ \gamma_{xy}\} \begin{Bmatrix} M_x \\ M_y \\ M_{xy} \end{Bmatrix} \quad (2)$$

$$\boldsymbol{\sigma}_{ij} \mathbf{S}_{ijkl} \boldsymbol{\sigma}_{kl} = \begin{Bmatrix} M_x \\ M_y \\ M_{xy} \end{Bmatrix} \begin{Bmatrix} S_{xx \ xx} & S_{xx \ yy} & S_{xx \ xy} \\ S_{yy \ xx} & S_{yy \ yy} & S_{yy \ xy} \\ S_{xy \ xx} & S_{xy \ yy} & S_{xy \ xy} \end{Bmatrix} \begin{Bmatrix} M_x \\ M_y \\ M_{xy} \end{Bmatrix} \quad (3)$$

2.1 The Hellinger-Reissner mixed variational dynamic formulation

The Hellinger-Reissner (HR) mixed functional [42, 65, 66, 67] expressed for dynamics problems may equate to the regular Lagrangian used in dynamics, but computed with mixed component. Basically, it means that the potential energy and the kinetic energy are calculated with both displacement and stress fields whenever possible. In this way, the HR dynamic functional can be given in its weak form as follows:

$$\Pi_{HRD} = \iiint_V -\boldsymbol{\sigma}_{ij} \mathbf{e}_{ij}(\mathbf{u}_i) + \frac{1}{2} \boldsymbol{\sigma}_{ij} \mathbf{S}_{ijkl} \boldsymbol{\sigma}_{kl} + \mathbf{b}_i \mathbf{u}_i + \frac{1}{2} \rho \dot{\mathbf{u}}_i^2 \, dV \quad (4)$$

considering $\boldsymbol{\sigma}_{ij}$ the stress, \mathbf{u}_i the displacement, $\mathbf{e}_{ij}(\mathbf{u}_i)$ the strain function of the displacement \mathbf{u}_i , \mathbf{b}_i the body force, ρ the volumic mass and \mathbf{S}_{ijkl} the elastic compliance matrix. The stationary condition or Euler-Lagrange equation can then be applied to the functional so as to conventionally solve a dynamic structure problem. We consider 3 main fields in the function:

- Mixed strain energy: $\sigma_{ij}e_{ij}(\mathbf{u}_i) - \frac{1}{2}\sigma_{ij}\mathbf{S}_{ijkl}\sigma_{kl}$
- Body force work: $\mathbf{b}_i\mathbf{u}_i$
- Kinetic energy: $\frac{1}{2}\rho\dot{\mathbf{u}}_i^2$

2.2 Mixed finite element for Kirchoff-Love Thin Plates

2.2.1 Definition of the Kirchoff-Love theory

The KL theory [63] is a thin plate theory that only focus on bending and twisting phenomenons, and doesn't take into consideration shearing effects. In this case, the displacement is given by:

$$\mathbf{u}_i = \begin{Bmatrix} w \\ \theta_x \\ \theta_y \end{Bmatrix} = \begin{Bmatrix} w \\ \frac{\partial w}{\partial y} \\ -\frac{\partial w}{\partial x} \end{Bmatrix} \quad (5)$$

considering w the transverse displacement, θ_x and θ_y the normal rotation around the -x and -y axis. The theory of KL is C^1 continuous on the node displacement, and assumes that the 2 rotations θ_x and θ_y depend on the transverse displacement w . It doesn't take into consideration any shearing phenomenon.

The strain is given by:

$$\mathbf{e}_{ij} = \begin{Bmatrix} \epsilon_{xx} \\ \epsilon_{yy} \\ \gamma_{xy} \end{Bmatrix} = \mathbf{D} \mathbf{u}_i \quad (6)$$

where \mathbf{D} is the operator

$$\mathbf{D} = \begin{Bmatrix} 0 & 0 & \frac{\partial}{\partial x} \\ 0 & -\frac{\partial}{\partial y} & 0 \\ 0 & \frac{\partial}{\partial x} & \frac{\partial}{\partial y} \end{Bmatrix} \quad (7)$$

The generalized stress field is given by:

$$\boldsymbol{\sigma}_{ij} = \begin{Bmatrix} M_x \\ M_y \\ M_{xy} \end{Bmatrix} \quad (8)$$

where $\{M_x, M_y, M_{xy}\}^T$ represents the bending and twisting moments. The transverse shearing force is not taken into consideration using the Kirchoff-Love theory.

The elastic compliance matrix is given by:

$$\mathbf{S}_{ijkl} = \begin{Bmatrix} \frac{12}{Et^3} & -\frac{12\nu}{Et^3} & 0 \\ -\frac{12\nu}{Et^3} & \frac{12}{Et^3} & 0 \\ 0 & 0 & \frac{24(1+\nu)}{Et^3} \end{Bmatrix} \quad (9)$$

where E is the Young Modulus, t is the thickness of the plate element and ν is the Poisson ratio. It is important to notice the elastic compliance matrix already contain the integration of the thickness of the plate, hence the appearance of the thickness in it and the use of generalized stress instead of stress.

The positive directions of the generalized stress field are shown in Figure 1.

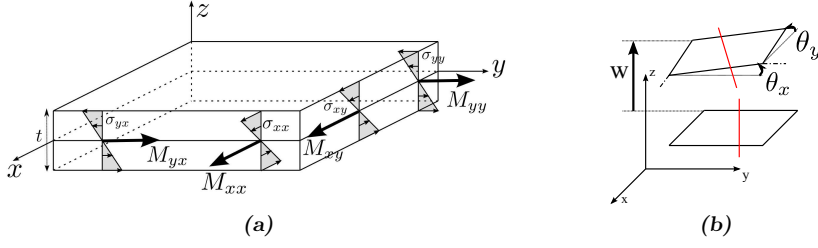


Fig. 1: Kirchhoff-Love theory (a) Generalized stresses (b) Displacements

2.2.2 Interpolation of nodal displacement in element

The features of the KL let us the choice between triangular and quadrilateral elements. In fact, the C^1 nodes displacement continuity conditions that link the displacement fields inside the plate (see equation 5) give us 9 conditions for each shape functions when using a 3-node triangular element, and 12 when using a 4-node quadrilateral and thus third degrees functions in both case. It is to be noted that our model fulfill the nodal displacement continuity but doesn't attend the edges continuity. The 3-node element option is preferred for the sake of simplicity and meshing simplicity. We assume that w , θ_x and θ_y , for a 3-node triangular element, are interpolated in terms of nodal displacements $\{w_i \theta_{xi} \theta_{yi}\}$ ($i = 1,2,3$), as follows:

$$w(x, y) = \sum_{i=1}^3 N_i(x, y) w_i \quad (10)$$

$$\theta_x(x, y) = \sum_{i=1}^3 \frac{\partial N_i(x, y)}{\partial y} \theta_{xi} \quad (11)$$

$$\theta_y(x, y) = \sum_{i=1}^3 -\frac{\partial N_i(x, y)}{\partial x} \theta_{yi} \quad (12)$$

Which gives us:

$$\mathbf{u}_i = \begin{Bmatrix} w \\ \theta_x \\ \theta_y \end{Bmatrix} = \mathbf{N}\mathbf{U} = \begin{Bmatrix} N_1 & N_2 & \dots & N_9 \\ \frac{\partial N_1}{\partial y} & \frac{\partial N_2}{\partial y} & \dots & \frac{\partial N_9}{\partial y} \\ -\frac{\partial N_1}{\partial x} & -\frac{\partial N_2}{\partial x} & \dots & -\frac{\partial N_9}{\partial x} \end{Bmatrix} \mathbf{U} \quad (13)$$

Chosing a 3-node triangular element, the shape functions have 9 conditions each and thus are 3rd order polynomials as follows:

$$N_i(x, y) = a_i + b_i x + c_i y + d_i xy + e_i x^2 + f_i y^2 + g_i x^3 + h_i y^3 + i_i (xy^2 + x^2 y) \quad (14)$$

2.2.3 Interpolation of stress

The order of the stress interpolation in function of the displacement interpolation has been discuss in the litterature [59,4], in particular for RM plates with the motivation of building shear-locking-free elements [70]. The choice of KL theory voluntarily avoids these discussions as it doesn't requires conditions as good as the RM theory needs. Thus, for the sake of simplicity, we assume that each field of the generalized stress is interpolated with linear functions and does not depend on the nodal values, which does not fulfill the C^0 nodes or edges continuity in terms of stresses. Each generalized stress is interpolated with 3 parameters β , as follows:

$$\begin{aligned} \boldsymbol{\sigma}_{ij} &= \begin{Bmatrix} M_x \\ M_y \\ M_{xy} \end{Bmatrix} = \mathbf{P}\boldsymbol{\beta} \\ \boldsymbol{\sigma}_{ij} &= \begin{Bmatrix} 1 & x & y & 0 & 0 & 0 & 0 & 0 & 0 \\ 0 & 0 & 0 & 1 & x & y & 0 & 0 & 0 \\ 0 & 0 & 0 & 0 & 0 & 0 & 1 & x & y \end{Bmatrix} \begin{Bmatrix} \beta_1 \\ \beta_2 \\ \cdot \\ \beta_9 \end{Bmatrix} \end{aligned} \quad (15)$$

These choices give us a total of 18 parameters per element matrix, as we have 9 displacement parameters U and 9 generalized stress parameters β .

2.2.4 Variational function and mixed finite element formulation

The HR mixed dynamic formulation presented in equation 4 can be discretized through equations 13 and 15, and express for a RM thick plate element as follows:

$$\begin{aligned} \Pi_{HRD} &= \iiint_V -\boldsymbol{\sigma}_{ij} \mathbf{e}_{ij}(\mathbf{u}_i) + \frac{1}{2} \boldsymbol{\sigma}_{ij} \mathbf{S}_{ijkl} \boldsymbol{\sigma}_{kl} + \mathbf{b}_i \mathbf{u}_i + \frac{1}{2} \rho \dot{\mathbf{u}}_i^2 \, dV \\ \Pi_{HRD} &= \iint_S \frac{1}{2} (\mathbf{N}\dot{\mathbf{U}})^T \mathbf{m} (\mathbf{N}\dot{\mathbf{U}}) - (\mathbf{P}\boldsymbol{\beta})^T (\mathbf{D}\mathbf{N}\mathbf{U}) \\ &\quad + \frac{1}{2} (\mathbf{P}\boldsymbol{\beta})^T \mathbf{S} (\mathbf{P}\boldsymbol{\beta}) \, dS + \iint_V b_i \mathbf{U} \, dS \end{aligned} \quad (16)$$

where

$$\mathbf{m} = \rho \begin{Bmatrix} t & 0 & 0 \\ 0 & \frac{t^3}{12} & 0 \\ 0 & 0 & \frac{t^3}{12} \end{Bmatrix} \quad (17)$$

ρ is the density and t the thickness.

The matrix development gives us:

$$\Pi_{RD} = \frac{1}{2} \dot{\mathbf{U}}^T \mathbf{M} \dot{\mathbf{U}} - \boldsymbol{\beta}^T \mathbf{G} \mathbf{U} - \boldsymbol{\beta}^T \mathbf{H} \boldsymbol{\beta} + \mathbf{F}^T \mathbf{U} \quad (18)$$

where

$$\mathbf{M} = \iint_S \mathbf{N}^T \mathbf{m} \mathbf{N} \, dS \quad (19)$$

$$\mathbf{G} = \iint_S \mathbf{P}^T \mathbf{D} \mathbf{N} \, dS \quad (20)$$

$$\mathbf{H} = \iint_S -\mathbf{P}^T \mathbf{S} P dS \quad (21)$$

and \mathbf{F} is the force vector applied to the mesh nodes.

Then we have:

$$\underbrace{\begin{Bmatrix} \mathbf{M} & \mathbf{0} \\ \mathbf{0} & \mathbf{0} \end{Bmatrix}}_{\mathbf{M}_{mix}} \begin{Bmatrix} \ddot{\mathbf{U}} \\ \ddot{\boldsymbol{\beta}} \end{Bmatrix} + \underbrace{\begin{Bmatrix} \mathbf{0} & \mathbf{G}^T \\ \mathbf{G} & \mathbf{H} \end{Bmatrix}}_{\mathbf{K}_{mix}} \begin{Bmatrix} \mathbf{U} \\ \boldsymbol{\beta} \end{Bmatrix} = \begin{Bmatrix} \mathbf{F} \\ \mathbf{0} \end{Bmatrix} \quad (22)$$

2.3 Convergence of the DM-FEM

In this subsection, we aim to show the convergence of the DM-FEM, on a dynamic point of view for the model we implemented. Many convergence studies are available in the literature for plate primal FEM for free vibrations or static problems, and plate mixed FEM for static analysis, but more rarely in dynamics and it's more likely depending on the interpolation, integration space and type of elements. That section is therefore necessary prior to the reduction subsection 3 which is the main point of this paper. The example we study in this part is a rectangular plate clamped on one edge and free on the three other edges (see figure 2). It is built with KL mixed triangular thin plate finite elements described in section 2. The plate is made of steel (see characteristics in table 1) and the thickness t of the plate is a variable of the different calculations, as well as the number of elements of the plate.

The first section of this part quickly reminds the convergence of the primal FEM compared to a reference (highly meshed primal FEM) prior to the second section that deals with the convergence of the DM-FEM compared to the dynamic primal FEM and the reference, considering the same number of elements in the plate. Both sections discuss two different thicknesses for each theory.

Table 1: Steel characteristics

Young Modulus (Pa)	2.1×10^{11}
Poisson ratio	0.33
Density ($kg.m^{-3}$)	7.5×10^3

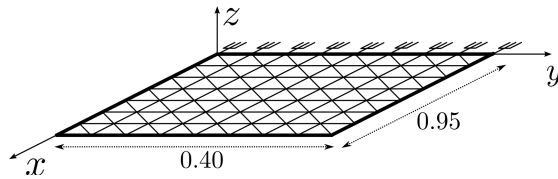


Fig. 2: Rectangular plate built with various triangular mixed plate elements

2.3.1 Convergence of the primal model

In this section, we focus on the convergence of the primal model compared to a reference. In fact, the next section 2.3.2 deals with the convergence between the DM-FEM and the primal dynamic FEM with the same meshes and theory. The convergence check is made with the relative error of the eigenfrequencies of the ten first modes, between the primal model and the reference. The relative error for the mode i is given by:

$$\epsilon_{i,\text{pri/ref}} = \frac{\text{abs}(f_{i,\text{primal}} - f_{i,\text{reference}})}{f_{i,\text{reference}}} \quad (23)$$

The results obtained with two different thicknesses of the plate (Table 2 and Table 3) show a good convergence. It appears that the characteristic size of the element doesn't influence the convergence of the model, as long as we stay in small thicknesses, as the KL theory defines it.

Table 2: Relative error $\epsilon_{i,\text{pri/ref}}$ for the first eigenfrequencies i for the example 1 with $t = 0.01m$ and Reissner KL mixed model

Mode	Elt	Element size (cm)			
		47.5	32.9	23.8	5.9
1	16	2.94	1.47	0.53	0.21
2	64	8.13	1.90	0.42	0.10
3	256	6.80	1.19	0.40	0.13
4	1024	-	7.58	1.63	0.33
5	-	-	2.87	0.24	0.06
6	-	-	11.59	2.28	0.41
7	-	-	1.72	0.01	0.01
8	-	-	4.90	0.27	0.00
9	-	-	3.35	0.06	0.00
10	-	-	20.35	3.29	0.43

2.3.2 Convergence of the mixed model towards the primal model

In this part, we focus on the convergence of the DM-FEM in comparison to the corresponding dynamic primal FEM with the same number of elements. The choice of showing the convergence of the dynamic primal FEM with a reference and then the DM-FEM to the primal corresponding FEM is the results of the analysis of this section: in fact, we show that the primal and mixed formulation show the exact same results with the interpolation and element setting we chose in section 2. Hence the interest of reminding the convergence of the primal formulation and then the mixed one with it.

The check procedure contains three parts. The first part is the relative error $\epsilon_{i,\text{mix/pri}}$ between the eigenfrequencies of the modes i of the dynamic primal FEM and the DM-FEM:

$$\epsilon_{i,\text{mix/pri}} = \frac{\text{abs}(f_{i,\text{mixed}} - f_{i,\text{primal}})}{f_{i,\text{primal}}} \quad (24)$$

Table 3: Relative error $\epsilon_{i,pri/ref}$ for the first eigenfrequencies i for the example 1 with $t = 0.001m$ and Reissner KL mixed model

Mode	Elt	Element size (cm)			
		47.5	32.9	23.8	5.9
1	16	3.16	2.11	1.05	0.00
2	64	8.14	1.67	0.42	0.00
3	256	6.68	1.17	0.33	0.00
4	1024	43.16	7.55	1.63	0.32
5		24.84	2.86	0.24	0.18
6		-	11.56	2.26	0.38
7		-	1.77	0.01	0.00
8		-	4.85	0.26	0.00
9		-	3.60	0.29	0.06
10		-	20.36	3.72	0.41

with $f_{i,mixed}$ the eigenfrequency of the mode i for the DM-FEM and $f_{i,primal}$ the eigenfrequency of the mode i for the primal FEM. The second part concerns the displacement shape of the modes and uses the Mac criterion as follows:

$$MAC(i, j) = \frac{(\mathbf{X}_i^T \mathbf{X}_j)^2}{(\mathbf{X}_i^T \mathbf{X}_i)(\mathbf{X}_j^T \mathbf{X}_j)} \quad (25)$$

with X_i the shape of the mode i of the primal FEM and X_j the shape of the mode j of the mixed FEM, taking into consideration only the displacement parameters. The third parameter deals with the stress convergence: it calculates a MAC-type criterion that compares the distribution of stress along the meshing with the primal and mixed model, as follows:

$$MAC_{stress}(i, j) = \frac{(\mathbf{Y}_i^T \mathbf{Y}_j)^2}{(\mathbf{Y}_i^T \mathbf{Y}_i)(\mathbf{Y}_j^T \mathbf{Y}_j)} \quad (26)$$

with respectively Y_i and Y_j the vector of the Von Mises stress on every node of the meshing, respectively for the mode i of the primal FEM and X_j the shape of the mode j of the mixed FEM.

We focus on a the largest frequency band possible depending on the convergence of the meshing. We choose to limit the study to a frequency band between 0 and $20kHz$ whenever it is possible. The convergence of the mixed FEM compared to that primal FEM appears to be dependent on the thickness of the plate, even though really good in both cases.

The results do not depend on the thickness of the plate. The three criteria concerning the eigenfrequencies 24, the form of the modes 25 and the stress distribution of the modes 26 are excellent for all the meshing tested, as:

$$\epsilon_{i,mix/pri} < 10^{-5} \quad (27)$$

$$MAC(i, i) \simeq 1 \quad (28)$$

$$MAC_{stress}(i, i) \simeq 1 \quad (29)$$

As those results are excellent, we decide to go further and calculate the relative error ϵ_{FRF} between a colocated FRF (see section 2.4) of the DM-FEM and the same colocated FRF of the corresponding primal FEM. Those results are shown in figure 4 (thickness $t = 1\text{cm}$) and figure 3 (thickness $t = 0.1\text{cm}$). Those graphics describe the relative error between two mixed and primal colocated FRF for various number of elements composing the plate (16(a), 64(b), 256(c), 410(d), 1024(e) and 4096(f) elements). The frequency band we study varies because of the convergence of the meshing. In fact, the smaller the thickness is, the lower the eigenfrequencies are, that is the reason why the highest mode described by the meshes is smaller than 20kHz . The results remain excellent, with a relative error between the two FRF less than 10^{-6} , with the thicknesses and numbers of elements studied. These outcomes reveals the fact that the DM-FEM and the dynamic primal FEM as described have exactly the same convergence and show almost identical results for the same meshing, which makes all the results from section 2.3.2 available for the DM-FEM as well.

So as to conclude this section, the calculations have shown that the KL thin plate theory does not depend on the thickness of the plate and have an excellent convergence. In the meantime, both the primal and mixed FEM (as discretized) show the same results in terms of eigenfrequencies, modal displacement, and Von Mises stress. It should be noted that other discretization options are available in the literature and may show a better convergence of the mixed FEM compared to the primal FEM in terms of stress, but this is not the main point of the article.

2.4 Features of the mixed model and consequences

2.4.1 Advantage

As explained in the introduction, mixed FEMs may present enormous benefits when it comes to Reissner-Mindlin thick plates analysis, stress continuity description and thin structure in general. In our case, the stress functions were voluntarily chosen simple, and the main interest kept for such model remains in the direct access to stresses among the plate structure. Indeed, such models provide the stress parameters in the response of the structure, whereas primal models must do extra calculation in order to get the stresses. This features leads to more facility to rebuild the stress field, and save CPU time. Table 4 gives an insight of the time gain with the mixed model for the computation of stress compared to the primal model. The calculations were made on the plate structure (figure 6) for the different meshing implemented in section 2.3. The time gain to rebuild the stress distribution within the structure is important as it remains between 45% and 11%. The gain appears to decrease as the size of the meshing increase because of the size of the matrices remains positive with the use of the mixed model.

Table 4: Time gain for the computation of Von Mises stress within the plate structure (figure 6) with the mixed model compared to the primal model

Elements	16	64	256	410	1024
Time Gain (stress on all structure)	45%	25%	19 %	15%	11%

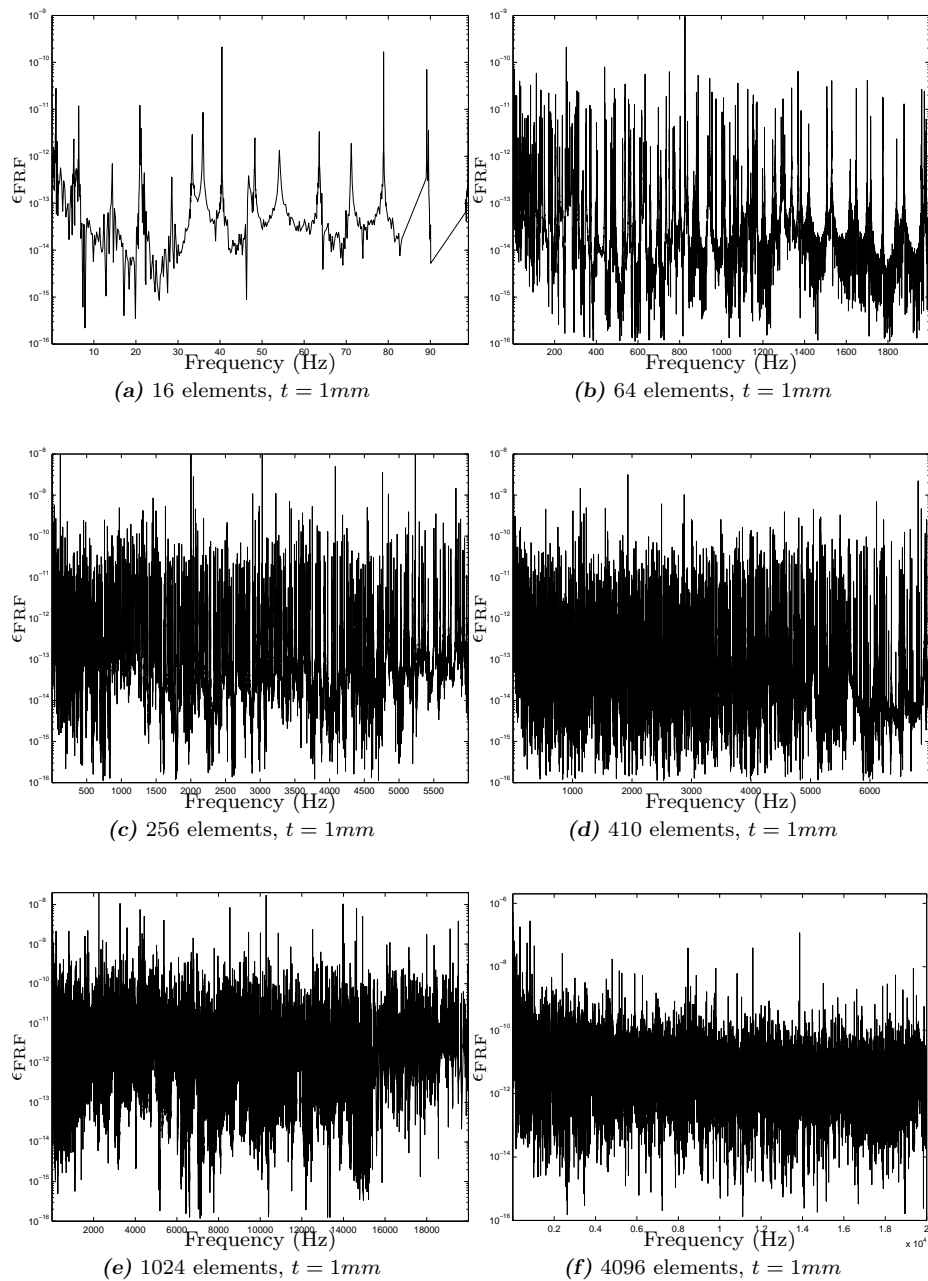


Fig. 3: Relative error on FRF ϵ_{FRF} , for $t = 0.1cm$ (a: 16 elements, b: 64 elements, c: 256 elements, d: 410 elements, e: 1024 elements, f: 4096 elements)

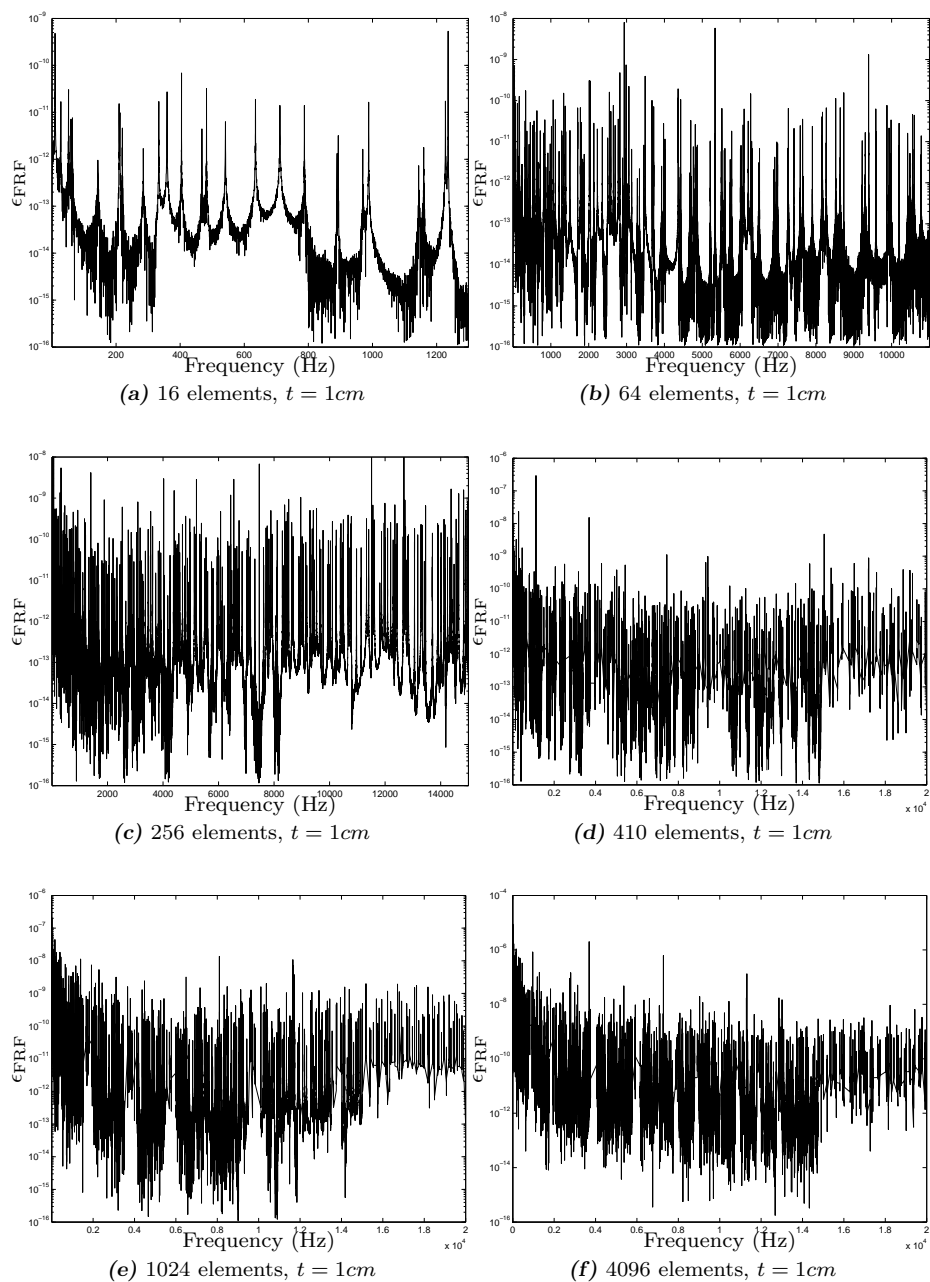


Fig. 4: Relative error on FRF ϵ_{FRF} , for $t = 1\text{cm}$ (a: 16 elements, b: 64 elements, c: 256 elements, d: 410 elements, e: 1024 elements, f: 4096 elements)

2.4.2 Inconveniences

Even though better for the description of stresses and faster to reach it, the mixed models presents some major drawbacks.

First of all, the number of DOFs of the elementary matrices is higher with mixed FEM than with primal FEM, due to the addition of stresses parameters. For the KL theory and discretization chosen, the size is twice bigger. As the assembly only links the displacement DOFs but leaves the generalized stress parameters unchanged, the ratio between primal and mixed model for concerning the DOFs is even bigger for an assembly. That inconvenience usually outweighs the stress access benefits because we may lose more time computing the response of the structure than we save reaching the stress. In that way, the present work aims at presenting a sub-structuring reduction method that offset this inconvenience and provides a smaller and faster model, both in terms of response and stress calculation.

Another drawback of the mixed model lies in its matrix formulation, due to empty part of the mass matrix in the stress field in 22. Thus, we cannot diagonalize the equations and use a regular modal synthesis method. Some methods presented in literature [58] consist in using the second line of the matrix system as a relation between displacement and stress, and thus build an "equivalent stiffness" \mathbf{K}_{eq} condensed on displacements. It is a quite simple way of solving an elastic dynamic mechanical mixed problem, and even save CPU time. But it only focuses on the displacements as a first result of the computation, it tends to lose the stress interest of the model and most of all, it doesn't fix the modal problem that remains impossible to get quickly. The main idea and choice of our work is to keep the matrix system as is, and make the computation, convergence test and reduction of the mixed model in its primary form, to get both displacements and stresses as a primary result.

A consequence of this feature: it is complicated to get a quick modal analysis with eigenfrequencies and mixed eigenvectors. We choose to build a Frequency Response Function (FRF) so as to get both eigenvalues and dynamic mixed response on a wide frequency band. We have to excite a degree of freedom with a harmonic force and observe the response as follows:

$$\begin{Bmatrix} \mathbf{U} \\ \boldsymbol{\beta} \end{Bmatrix} = (\mathbf{K}_{mix} - \omega^2 \mathbf{M}_{mix})^{-1} \begin{Bmatrix} \mathbf{F} \\ \mathbf{0} \end{Bmatrix} \quad (30)$$

with ω the chosen pulsation of the harmonic force and \mathbf{F} the force vector apply on the DOFs of the meshing. This calculation gives us the dynamic mixed response of the structure to a harmonic excitation with a pulsation ω , on the chosen DOF. So as to get a complete FRF on a frequency band, we must repeat it as many times as the number of frequencies we want in the FRF curve and choose a specific degree of freedom to observe (usually the same we observe). All the eigenfrequencies and the mixed mode form studied in this paper are computed through equation 30.

A second consequence of this feature: we cannot apply a regular primal modal synthesis method [48, 49] in order to reduce the model and increase the computation speed, as we cannot easily compute the mode on a mixed model. This is the reason why the reduction method presented in next section 3 is based on primal modes and doesn't require to get a proper modal analysis of the mixed model.

As a conclusion, the DM-FEM we implemented presents the same displacement and stress dynamic convergence as a primal FEM with the same meshing,

but provides a much faster access to the stress field. Nevertheless, its size is bigger may complicate the response computation, and it is impossible to use displacement modal analysis. These are the reason why we implement in the next section 3 a new sub-structuring reduction method that reduces the numerical size of the mixed model and using primal modes.

3 MODAL REDUCTION ON A MIXED FINITE ELEMENT MODEL

As described in the first section 2, the numerical sizes of the DM-FEM is significantly higher than primal models using the same theory and meshing. The elementary matrix is twice bigger. As an example, the clamped plate tested in section 2.3 composed of 1024 elements is composed by 3270 primal DOFs or 12486 mixed DOFs which is almost 4 times more. It is therefore important to reduce it in order to increase the computation speed. Not to mention that any reduction could also be useful for the RM thick plate theory that suffers from "shear-locking" problems. Nevertheless, the main point of this paper is to develop a general reduction method for mixed FEM

The distinctive feature of the mixed model (not condensed on the displacements) is the impossibility to apply a regular CMS method as the mixed matrices cannot be diagonalized. Thus, the idea of this part is to reduce the numerical size of the model, by adapting regular sub-structuring methods for primal FEM, easily computable, to DM-FEMs.

The sub-structuring methods using modal components permit to describe the low frequency phenomenon of a structure split into substructures using eigenmodes of each sub-structures and constraint modes to link them. The constraint modes permits to offset the truncation of the eigenmodes of each sub-structure, and thus increase the precision of the method. This section deals with one of these sub-structuring method, and its application to our DM-FEM.

The structure is supposed to be composed of two sub-structures, which does not restrict the method. A superscript $^{(s)}$ is added to make the distinction between each substructure s . The subscripts i and j refer to internal and junction DOFs respectively. The subscripts E refer to "fixed" eigenmodes. We may also add the subscript (U) and (β) when talking about a mixed formulation to refer to displacement fields and generalized stress field respectively.

3.1 Various sub-structuring methods

There are two main modal synthesis families. The first one is the fixed interface methods described in 1968 for the first time by Craig and Bampton [30,29]. It is based on eigenmodes of each substructure, assuming that the boundary is held fixed, and constraint static modes (these are substructure response to successive unit boundary displacement). The second family refers to free interface methods and has been released in 1971 for the first time by MacNeal [55]. It is based on eigenmodes of each substructure, assuming that the boundary is free and attachment modes (substructure response to successive unit boundary force). In this case, we are going to use a "fixed mode" method. It is important to notice that

the regular substructuring methods are applied to primal FEM with only one field (displacement), and that is the way we describe the "fixed mode" method in the next sections. The other sections deal with the application of those methods to our DM-FEM and the assembly of the substructures.

3.2 Fixed mode method

The regular modal synthesis using fixed modes keep a number of boundary modes equal to the number of junction DOFs. The constraint static modes represent the behavior of the structure regarding the interface, that is to say the response of the structure to successive unit boundary displacement). Considering two substructure a and b and a global structure s , the constraint static modes are computed as follows:

$$\Psi_s = \begin{Bmatrix} \Psi_i^{(a)} \\ \Psi_j \\ \Psi_i^{(b)} \end{Bmatrix} = \begin{Bmatrix} -\mathbf{K}_{ii}^{(a)-1} \mathbf{K}_{ij}^{(a)} \\ \mathbf{I}_{ij} \\ -\mathbf{K}_{ii}^{(b)-1} \mathbf{K}_{ij}^{(b)} \end{Bmatrix} \quad (31)$$

The fixed mode method is a primal method that separates, for each substructure (a), boundary DOFs $\mathbf{U}_j^{(a)}$ and internal DOFs $\mathbf{U}_i^{(a)}$. It projects the initial DOFs of the substructure (a) on a new smaller basis composed of truncated modal DOFs $\boldsymbol{\eta}_{FI}^{(a)}$ and the same boundary DOFs, as follows:

$$\begin{Bmatrix} \mathbf{U}_i^{(a)} \\ \mathbf{U}_j^{(a)} \end{Bmatrix} = \begin{Bmatrix} \boldsymbol{\Phi}_{FIi}^{(a)} & \Psi_i^{(a)} \\ \mathbf{0} & \mathbf{I}_{ij} \end{Bmatrix} \begin{Bmatrix} \boldsymbol{\eta}_{FI}^{(a)} \\ \mathbf{U}_j^{(a)} \end{Bmatrix} \quad (32)$$

where $\boldsymbol{\Phi}_{FI}^{(a)}$ is a truncated basis composed of eigenmodes of the structure a assuming that the boundary nodes are held fixed, and $\{\Psi_i^{(a)} \mathbf{I}_{ij}\}^T$ are the constraint static modes previously defined. Note that all the modes mentioned in this section are taken from the primal associated FEM with the same meshing

3.3 Projection of generalized stress field

The fixed mode method previously defined is primal methods. It projects the displacement degrees of freedom on a new basis, but they don't reduce the generalized stress parameters used in a mixed formulation.

Considering the second line of the equation 22, we can express the generalized stress parameters in function of the displacement parameters of of the corresponding stress, as follows:

$$\boldsymbol{\beta}^{(a)} = -(\mathbf{H}^{(a)})^{-1} \mathbf{G}^{(a)} \mathbf{U}^{(a)} \quad (33)$$

That idea was already mentionned earlier in the possibility of transforming the mixed FEM into a "condensed" primal FEM. In our case, that method is only used for the reduction. Indeed, the projection of the generalized stress on a primal base composed of fixed mode can now be express as follows:

$$\boldsymbol{\beta}^{(a)} = \begin{Bmatrix} \mathbf{P}^{(a)} \begin{Bmatrix} \boldsymbol{\Phi}_{FIi}^{(a)} \\ \mathbf{0} \end{Bmatrix} & \mathbf{P}^{(a)} \begin{Bmatrix} \Psi_i^{(a)} \\ \mathbf{I}_{ij} \end{Bmatrix} \end{Bmatrix} \begin{Bmatrix} \boldsymbol{\eta}_{FI}^{(a)} \\ \mathbf{U}_j^{(a)} \end{Bmatrix} \quad (34)$$

where $\mathbf{P}^{(a)} = -(\mathbf{H}^{(a)})^{-1} \mathbf{G}^{(a)}$.

3.4 Application to the mixed model

So as to apply the substructuring methods to our DM-FEM, we can choose to project the displacement field and generalized stress field in two different way, that is to say with different method and/or different truncation. In this article we decide to project the displacement on a basis composed of fixed modes and the generalized stress on another basis composed of fixed modes (but possibly with different truncation). The reduction of the whole substructure a is given by:

$$\begin{Bmatrix} \mathbf{U}_i^{(a)} \\ \mathbf{U}_j^{(a)} \\ \boldsymbol{\beta}^{(a)} \end{Bmatrix} = \mathbf{T}^{(a)} \begin{Bmatrix} \boldsymbol{\eta}_{FI(U)}^{(a)} \\ \boldsymbol{\eta}_{FI(\beta)}^{(a)} \\ \mathbf{U}_j \end{Bmatrix} \quad (35)$$

where

$$\mathbf{T}^{(a)} = \begin{Bmatrix} \boldsymbol{\Phi}_{FIi(U)}^{(a)} & \mathbf{0} & \boldsymbol{\Psi}_i^{(a)} \\ \mathbf{0} & \mathbf{0} & \mathbf{I}_{ij} \\ \mathbf{0} & \mathbf{P}^{(a)} \begin{Bmatrix} \boldsymbol{\Phi}_{FIi(\beta)}^{(a)} \\ \mathbf{0} \end{Bmatrix} & \mathbf{P}^{(a)} \begin{Bmatrix} \boldsymbol{\Psi}_i^{(a)} \\ \mathbf{I}_{ij} \end{Bmatrix} \end{Bmatrix} \quad (36)$$

where (U) and (β) are subscripts respectively for displacement parameters and generalized stress parameters. In this case, it is also important to notify the difference between the eigenmodes used for the displacement projection and the ones used for the stress parameters, even though the method is the same and the full eigenmodes matrices is the same, because the truncation may be different.

It should be noted as well that, the projection using some eigenmodes of the primal equivalent FEM, our method requires to build both primal and mixed assemblage at the same time for each structure we study, as all the reduction of the mixed FEM comes from the primal associated FEM. Of course, both models use the same theory and same meshing to link them together.

3.5 Assembly

We assemble the substructures a and b considering:

$$\mathbf{U}_j^{(a)} = \mathbf{U}_j^{(b)} = \mathbf{U}_j \quad (37)$$

Then, the assembly may lead to different formulation depending on the method we use (fixed or free mode method) for the projection of the displacement field. For the "fixed mode" method used here, the reduction of the assembly of the structure $(a + b)$ is then given by:

$$\begin{Bmatrix} \mathbf{U}_i^{(a)} \\ \mathbf{U}_j^{(a)} \\ \mathbf{U}_i^{(b)} \\ \boldsymbol{\beta}^{(a)} \\ \boldsymbol{\beta}^{(b)} \end{Bmatrix} = \mathbf{T} \begin{Bmatrix} \boldsymbol{\eta}_{FI(U)}^{(a)} \\ \boldsymbol{\eta}_{FI(\beta)}^{(b)} \\ \mathbf{U}_j \\ \boldsymbol{\eta}_{FI(U)}^{(a)} \\ \boldsymbol{\eta}_{FI(\beta)}^{(b)} \end{Bmatrix} \quad (38)$$

where

$$T = \begin{pmatrix} \Phi_{FII(U)}^{(a)} & \mathbf{0} & \Psi_i^{(a)} & \mathbf{0} & \mathbf{0} \\ \mathbf{0} & \mathbf{0} & I_{ij} & \mathbf{0} & \mathbf{0} \\ \mathbf{0} & \mathbf{0} & \Psi_i^{(b)} & \Phi_{FII(U)}^{(b)} & \mathbf{0} \\ \mathbf{0} & P^{(a)} \begin{Bmatrix} \Phi_{FII(\beta)}^{(a)} \\ \mathbf{0} \end{Bmatrix} & P^{(a)} \begin{Bmatrix} \Psi_i^{(a)} \\ I_{ij} \end{Bmatrix} & \mathbf{0} & \mathbf{0} \\ \mathbf{0} & \mathbf{0} & P^{(b)} \begin{Bmatrix} \Psi_i^{(b)} \\ I_{ij} \end{Bmatrix} & \mathbf{0} & P^{(b)} \begin{Bmatrix} \Phi_{FII(\beta)}^{(b)} \\ \mathbf{0} \end{Bmatrix} \end{pmatrix} \quad (39)$$

The figure 5 summarises the calculation of the dynamic response with the use of the sub-structuring method (the subscripts *pri*, *mix* and *red* representing respectively the primal, mixed, and mixed reduced matrix).

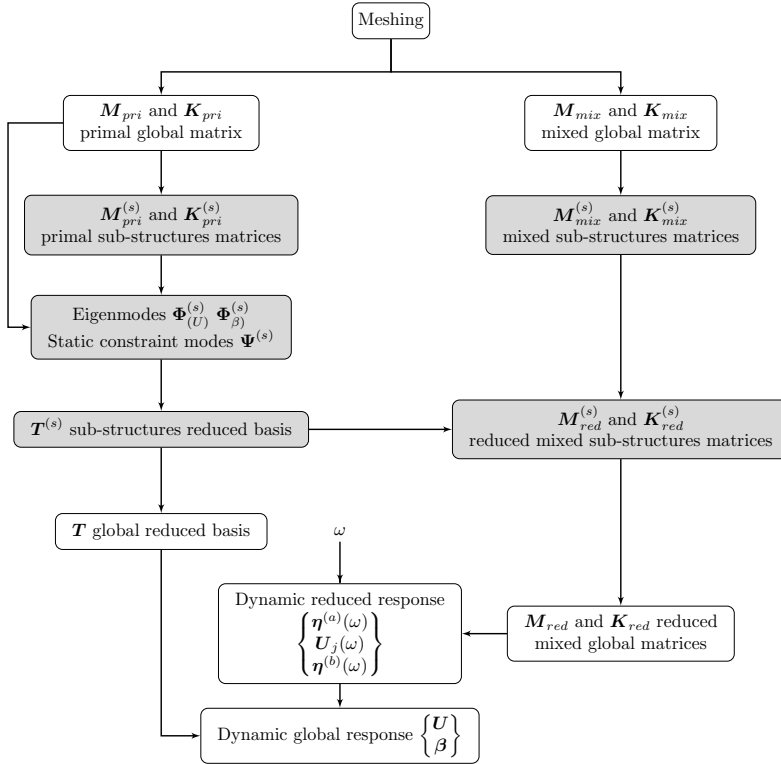


Fig. 5: Computation of the dynamic response of the global structure using the sub-structuring method (global structure level, sub-structure level. Each block needs all the input to be computed

In the next section, we use a simple example with two substructures to check the convergence of this method in function of the truncation of the eigenmodes chosen.

4 CONVERGENCE STUDY OF THE REDUCTION

4.1 Example

This section focus on the convergence of DM-FEM described in 2, using the method described in section 3, depending on the number of modes kept in the truncation for displacement fields and generalized stress fields. The example used in this part is composed of two different plates, meshed with KL triangular DM-FEM described in section 2. It is made of steel (see characteristics in table 1) and we choose a thickness of $1e^{-3}m$. That example is shown in figure 6.

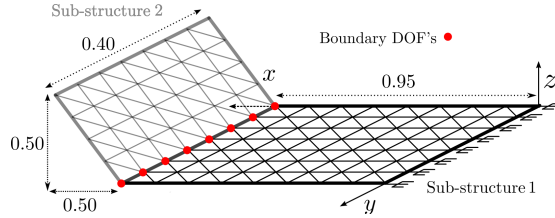


Fig. 6: Double structured thin plate built with KL triangular mixed elements

The global structure is composed of 922 elements whilst the first plate is composed of 414 elements and the second plate of 510 elements. The first plate is clamped on one edge (102 DOFs clamped) and the junction is composed of 102 boundary DOFs. The table 5 summarise the elements and DOFs characteristics of the test structure and substructures.

Table 5: Characteristics of the test structure for the convergence study of the reduction

Plate	Elements	DOFs	displacement DOFs	Generalized stress DOFs	Boundary DOFs
Global structure	922	11256	2958	8298	/
Sub-structure 1	414	5064	1338	3726	102
Sub-structure 2	510	6294	1722	4572	102

In this section, we calculate the results of the dynamic response of the global structure with the sub-structuring method (see section 3) for different truncations (see Table 6).

Table 6: Different truncations for the sub-structuring method (number of modes per substructure)

Name	5-5	10-10	20-20	40-40	60-60	80-80	100-100	150-150	Reference
U modes	5	10	20	40	60	80	100	150	2958
β modes	5	10	20	40	60	80	100	150	8298
Boundary DOFs						102			

4.2 Checking Method

This section focus on the convergence of the reduced DM-FEM in comparison to the DM-FEM with no reduction (considering that the DM-FEM has already converged with the meshing). We calculate the dynamic response of the global structure with the sub-structuring method (see section 3) and for different truncations, and compare it to the non-reduced dynamic response. The check procedure contains two parts. The first part concerns the relative error between the eigenfrequencies of each mode i of the global structure as described in the following equation:

$$\epsilon_{i,\text{red/mix}} = \frac{\text{abs}(f_{i,\text{mixed reduced}} - f_{i,\text{mixed}})}{f_{i,\text{mixed}}} \quad (40)$$

with $f_{i,\text{mixed}}$ the eigenfrequency of the mode i for the DM-FEM and $f_{i,\text{mixed reduced}}$ the eigenfrequency of the mode i for the reduced DM-FEM. The second part concerns the shape of the modes and uses the Mac criterion with both displacement and stress parameters as follows:

$$\text{MAC}(i, j) = \frac{(\mathbf{X}_i^T \mathbf{X}_j)^2}{(\mathbf{X}_i^T \mathbf{X}_i)(\mathbf{X}_j^T \mathbf{X}_j)} \quad (41)$$

with X_i the shape of the mode i of the DM-FEM and X_j the shape of the mode j of the reduced DM-FEM.

The results are shown as graphics describing the relative error (equation 40) on the eigenfrequencies in function of the mode i and compare it to an arbitrary limit of 3%. Each marker gives an insight of the MAC criterion (equation 41) of the mode i , as follows:

- black marker: $\text{MAC} \geq 0.8$ ("good" criterion)
- grey marker: $0.5 \leq \text{MAC} < 0.8$ ("medium" criterion)
- white marker: $\text{MAC} < 0.5$ ("bad" criterion)

We also show the matrices of the MAC criterion for each sub-structuring method and truncation, to focus on the form of the modes. The idea is to compare the number of modes used in the truncations of the displacement field basis and the generalized stress field basis, and the number of modes well defined (frequency and form) by the corresponding mixed reduced model.

4.3 Results: truncation of the displacement and stress modes

The table 6 summarises the various truncations we tested for the sub-structuring method (see section 3) and compares them to the non-reduced method parameters.

The results are shown in figures 7 and 8 (relative error and insight of the MAC criterion) and figures 9 and 10 (matrix of the MAC criterion). The different truncations are explained in table 6.

The results for this method are promising. In fact, they look like the results we would get with a sub-structuring method applied on a primal model, with a good representation for low frequency and a convergence limit frequency that increases with the number of modes kept in the truncation. It appears that, most of the time, the two check criteria work together as they are both "good" or "bad" at the same time, that is to say MAC criterion and frequency error are getting bad at the same time when the model is diverging.

Nevertheless, depending on the truncation and number of modes we can possibly observe, it sometimes remains a few modes with one of the two criteria (or sometimes both) that are "medium" or even "bad" for some modes, but they are very rare and exceptions among many other well described modes. We call them "singular modes". The table 7 summarise the frequency and mode bands well defined by the sub-structuring method and the number and density of "singular modes" among that band.

Table 7: Results for different truncation, using the sub-structuring method

Name	5-5	10-10	20-20	40-40	60-60	80-80	100-100	150-150	Ref mixed	Primal
Relative error figure	7a	7b	7c	7d	7e	7f	8a	8b	/	/
MAC figure	9a	9b	9c	9d	9e	9f	10a	10b	/	/
Limit mode	12	22	41	76	113	147	181	276	/	/
Limit frequency (Hz)	33	70	146	290	447	580	730	1170	/	/
Nb of singular modes	0	0	1	2	6	4	3	10	/	/
% of singular modes	0	0	2.4	2.6	5.3	2.7	1.7	3.6	/	/
Number of DOFs	122	142	182	262	342	422	502	702	11256	2958
Acces to stress	Yes	Yes	Yes	Yes	Yes	Yes	Yes	Yes	Yes	No

The results shown in table 7 are good, and reveal the fact that we can highly decrease the number of DOFs but still keep a good convergence on a large band of modes. For example, the "20-20" reduction reduce the DOFs from 11256 to 182 (more than 60 times less) and allows a good representation of the dynamic response for the 42 first modes, with only two singular modes (with a "medium" MAC criterion: $0.5 \leq MAC < 0.8$).

As the frequency band depends on the thickness of the plate, it sounds more likely to talk about a number of modes observable instead of a frequency band. In fact, the same computation with a higher thickness gives the same results in terms of modes, but a higher frequency band because the higher the thickness is, the higher the eigenfrequencies are.

The figure 11 shows the von mises stress distribution in the global structure for the 12th mode, using the sub-structuring method (see section 3) with the truncation "5-5". In this case, the 12th mode is the last one we can clearly observe among the frequency band.

Despite the good results of this method, we can still notice the presence of some "singular" modes (with a "medium" or "bad" criterion) among the frequency band we observe. It seems that some modes needs a specific higher frequency mode to be well represented, but that phenomenon concerns no more than 5% of the repre-

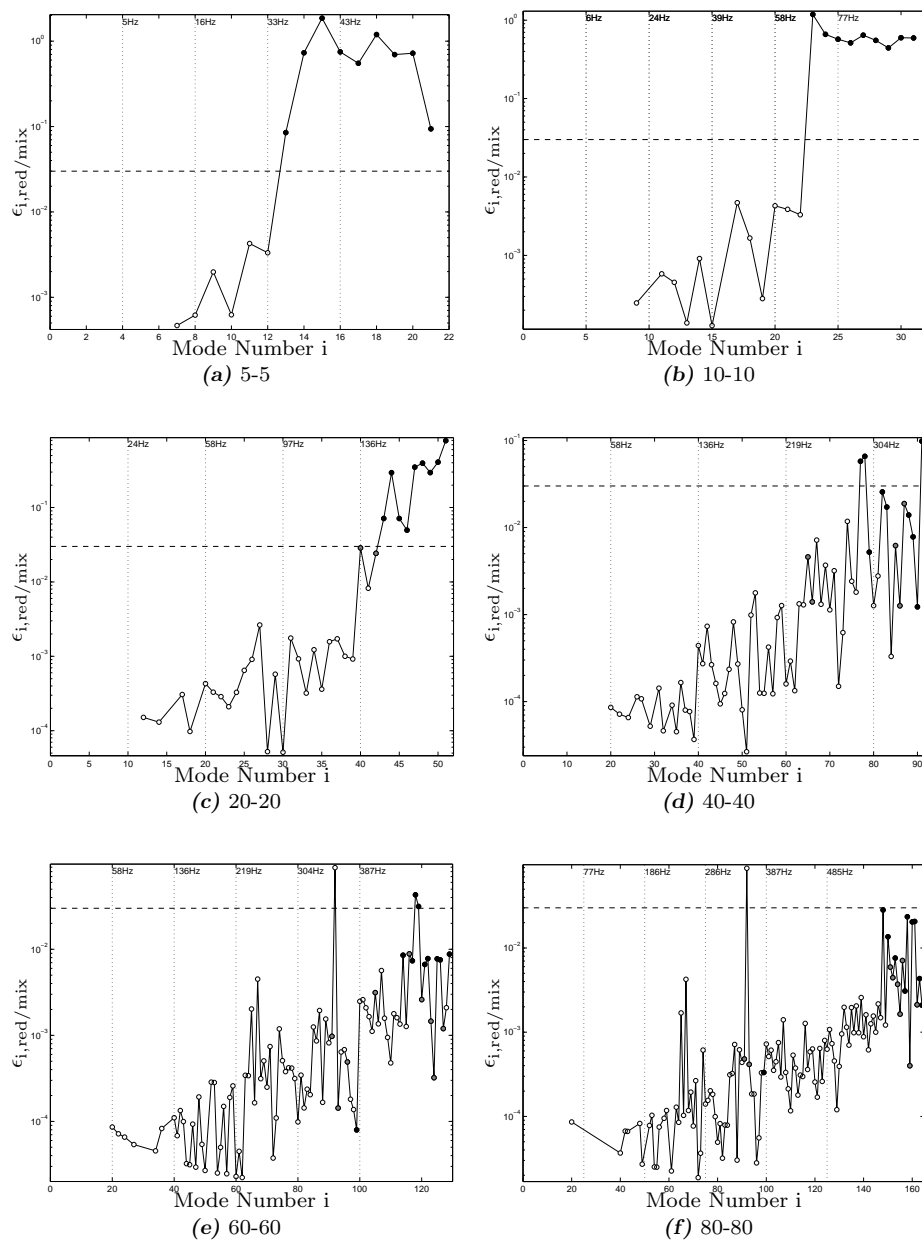


Fig. 7: Relative error on the eigenfrequencies $\epsilon_{i,\text{red}/\text{mix}}$ in function of the mode i and insight of the MAC criterion for each modes (truncations: a:5-5, b:10-10, c:20-20, d:40-40, e:60-60, f:80-80)

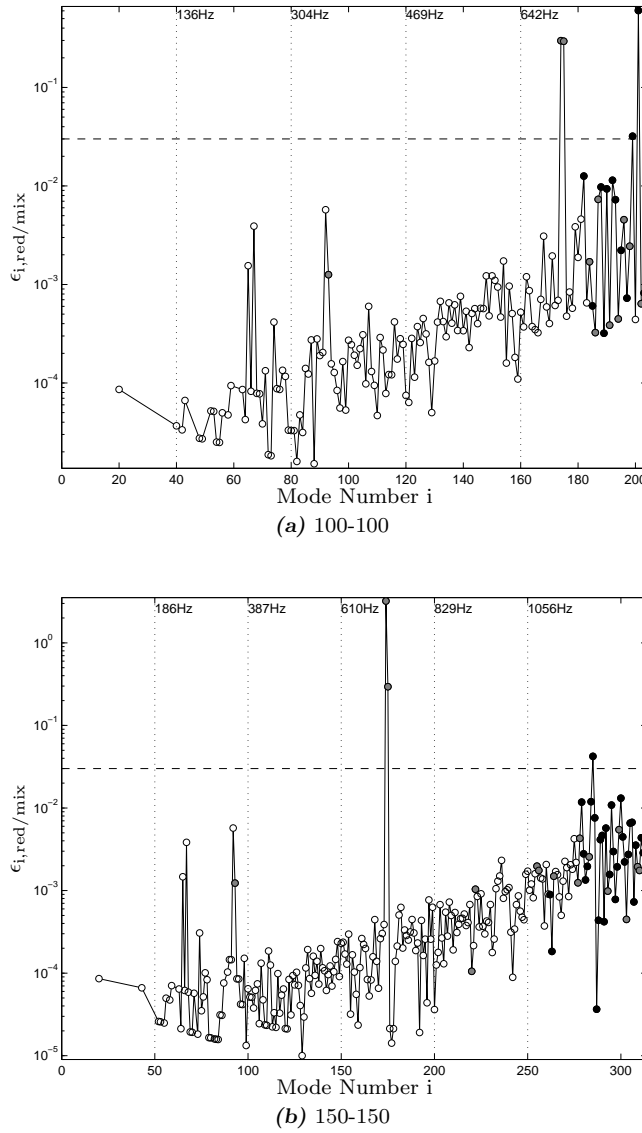


Fig. 8: Relative error on the eigenfrequencies $\epsilon_{i,\text{red}/\text{mix}}$ in function of the mode i and insight of the MAC criterion for each modes (truncations: a:100-100, b:150-150)

sented modes most of the time. Furthermore, those singularities tend to disappear or change with different meshes, which could explain that the method is not responsible for the singularities. It looks like the presence of singularities is random, but does not really question the quality of this reduction.

Even though there is no exact rule to predict the mode band we can observe in function of the truncation, we understand that, generally, it corresponds to a

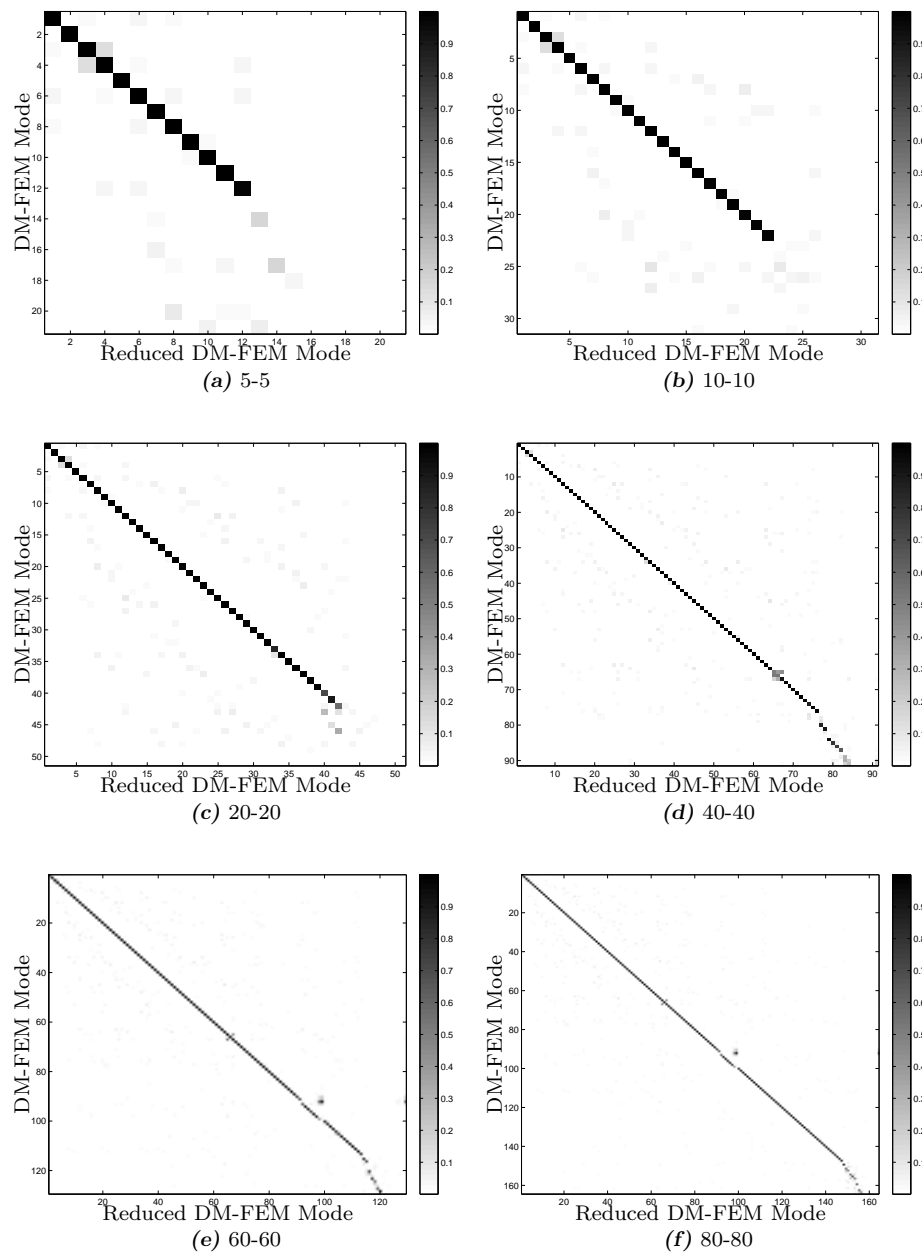


Fig. 9: MAC criterion for each modes (truncations: a:5-5, b:10-10, c:20-20, d:40-40, e:60-60, f:80-80)

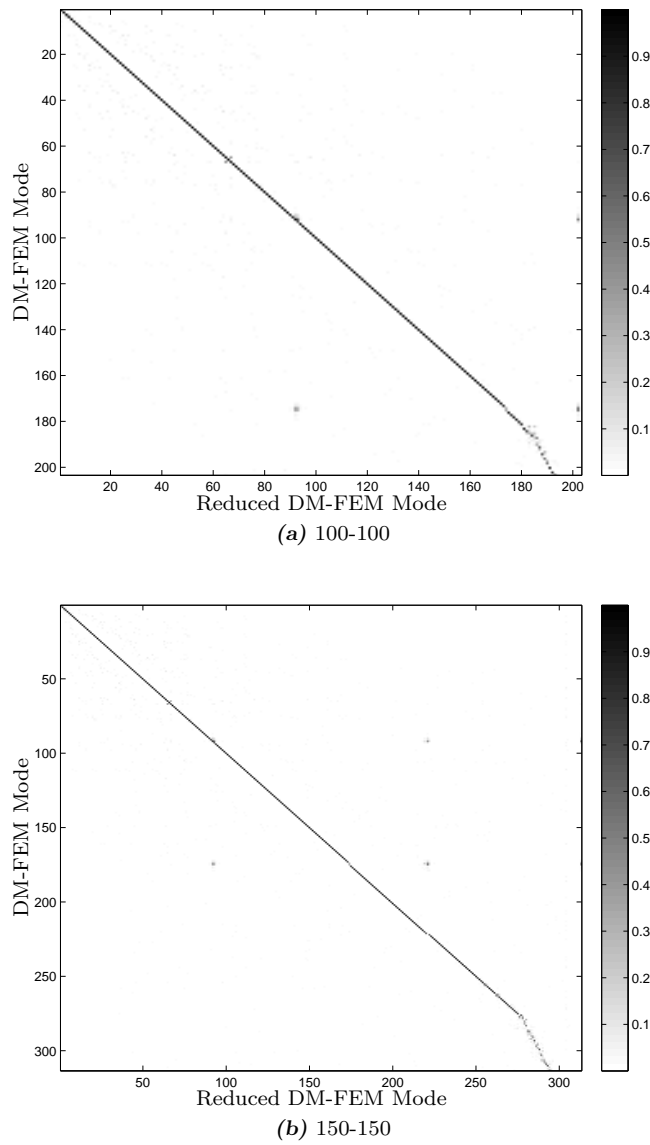


Fig. 10: MAC criterion for each modes (truncations: a:100-100, b:150-150)

number of modes equal or a bit inferior to the sum of the displacement modes and generalized stress modes for each substructure. We also observe that the amount of "singular mode" tend to increase with the frequency band we can observe, but this remains rather random, and does not influence the global convergence frequency band.

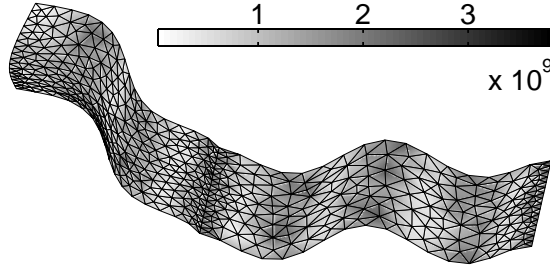


Fig. 11: Von Mises stress distribution in the 2 plates for the 12th mode ($f = 33.1\text{Hz}$) obtained with the reduction method, truncation "5-5"

5 CONCLUSIONS

As a first step, we implement a DM-FEM for KL theory and discuss its convergence prior to the reduction. The computation reveals that, as long as the primal model converges to a reference solution, the mixed one (with the same amount of elements) also converges to the same reference. It basically means that the mixed model has the same convergence as the regular primal model associated for the simple interpolation and element type we chose. When choosing the KL thin plate theory, the FEM has a great convergence, requires a low amount of element to reach the reference and the results does not depend on the thickness of the plate when sticking to small thicknesses.

The advantage of this formulation is the easy access to the stress within the plate as a primary result of an analysis, without any other calculation. The first disadvantage is the numerical size of the mass and stiffness matrices that is much bigger as they use parameters for the generalized stress fields, that is why we aim at reducing the finite element model. Nevertheless, the second drawback is the impossibility to diagonalize them as they are, which force us to imagine different methods. Indeed, the article presents a new reduction method applicable to DM-FEMs in general. The difficulty in using regular displacement CMS methods and sub-structuring methods leads us to a different reduction. In fact, the idea is to adapt a displacement sub-structuring modal reduction to the mixed model by separating the projection of displacement and generalized stress. The primal model associated uses the same meshing and same theory as the mixed model. With the method presented in this paper, we reduce the mixed model using a basis composed of "fixed interface modes" obtained with a Craig & Bampton method and the generalized stress field on another projected basis also composed of "fixed interface modes". The results shown in the last section are good and permit to decrease a lot the number of DOFs, and still keep a good convergence on a large frequency band, despite the presence of singularities among that band. The convergence may change depending on the structure and the type of junction but we can still set the fact that, for the example chosen, we can divide the number of DOFs by 22, 32 and 62 and keep a good representation of the 181, 113 and 41

first modes respectively. In the end, we dispose of a reduced mixed finite element model for thin plate that keeps the advantages of that theory meanwhile getting rid of its main inconvenients.

AKNOWLEDGEMENT

The first author gratefully acknowledges the French Education Ministry which supports this research.

References

1. J.H. Argyris. Continua and discontinua. Proc. Conf. Matrix Meth. Struct. mech., pages 11–190, 1965.
2. D.N. Arnold, F. Brezzi, and J.Jr. Douglas. Peers: A new mixed finite element for plane elasticity. Japan Journal of Applied Mathematics, 1(2):347–367, 1984.
3. D.N. Arnold and R.S. Falk. A new mixed formulation for elasticity. Numerische Mathematik, 53(1-2):13–30, 1988.
4. D.N. Arnold and R. Winther. Mixed finite element for elasticity in the stress-displacement formulation. 329:33–42, 2003.
5. R. Ayad, G. Dhatt, and J.L. Batoz. A new hybrid variational approach for reissner-mindlin plates. the misp model. International Journal For Numerical Methods in Engineering, 42:1149–1179, 1998.
6. I. Babuska. The finite element method with lagrangian multipliers. Numerische Mathematik, 20(3):179–192, 1973.
7. K.J. Bathe and E.N. Dvorkin. Short communication a four-node plate bending element based on mindlin/reissner plate theory and a mixed interpolation. International Journal For Numerical Methods in Engineering, 21:367–383, 1985.
8. K.J. Bathe and E.N. Dvorkin. A formulation of general shell elements - the use of mixed interpolation of tensorial components. International Journal For Numerical Methods In Engineering, 22:697–722, 1986.
9. A. Benjeddou. Advances in piezoelectric finite element modeling of adaptative structural elements: a survey. Computers and Structures, 76:347–363, 2000.
10. A. Benjeddou and O. Andrianarison. A thermopiezoelectric mixed variational theorem for smart, multilayered composites. Computers and Structures, 83:1266–1276, 2005.
11. S. Besset and L. Jézéquel. Dynamic sub-structuring based on a double modal analysis. Journal of Vibration and acoustics, 130(1):011008, 2008.
12. K.U. Bletzinger, M. Bischoff, and E. Ramm. A unified approach for shear-locking-free triangular and rectangular shell finite element. Computers and Structures, 75:321–334, 2000.
13. F. Brezzi. On the existence, uniqueness and approximation of saddle-point problems arising from lagrangian multipliers. Revue Francaise d’Automatique, informatique, rechefceh opérationnelle, analyse numérique, 8(2):129–151, 1974.
14. D. Brizard, L. Jézéquel, S. Besset, and B. Troclet. Determinantal method for locally modified structures. application to the vibration damping of a space launcher. Computational Mechanics, 20:631–644, 2012.
15. J. Bron and G. Dhatt. Mixed quadrilateral elements for bending. AIAA Journal, 10:1359–1361, 1972.
16. E. Carrera. An improved reissner-mindlin-type model for the electromechanical analysis of multilayered plates including piezo-layers. Journal of Intelligent Materials Systems and Structures, 8:232–248, 1997.
17. E. Carrera. Evaluation of layerwise mixed theories for laminated plate analysis. AIAA Journal, 36:830–839, 1998.
18. E. Carrera. An assesment of mixed and classical theories for the thermal stress analysis of orthotropic multilayered plates. Journal of Thermal Stresses, 23:797–831, 2000.
19. E. Carrera. Developments, ideas, and evaluations based upon reissner’s mixed variational theorem in the modeling of multilayered plates and shells. Applied Mechanics Reviews, 54:301–329, 2001.
20. E. Carrera and M. Boscolo. Classical and mixed finite element for static and dynamic analysis of piezoelectric plates. International Journal For Numerical Methods In Engineering, 70:1135–1181, 2007.

21. E. Carrera and L. Demasi. Classical and advanced multilayered plate elements based upon pvd and rmvt. part 1: Derivation of finite element matrices. International Journal For Numerical Methods in Engineering, 55:191–231, 2002.
22. E. Carrera and L. Demasi. Classical and advanced multilayered plate elements based upon pvd and rmvt. part 2: Numerical implementation. International Journal For Numerical Methods in Engineering, 55:253–291, 2002.
23. A. Chatterjee and A.V. Setlur. A mixed finite element formulation for plate problems. International Journal For Numerical Methods In Engineering, 4:67–84, 1972.
24. M. Cho and R. Parmerter. Efficient higher order composite plate theory for general lamination configurations. AIAA Journal, 31(7):1299–1306, 1993.
25. O Civalek. Application of differential quadrature (dq) and harmonic differential quadrature (hdq) for buckling analysis of thin isotropic plates and elastic columns. Engineering Structures, 26:171–186, 2004.
26. O Civalek. Three-dimensional vibration, buckling and bending analyses of thick rectangular plates based on discrete singular convolution method. International Journal of Mechanical Sciences, 49:752–765, 2007.
27. O Civalek. Free vibration analysis of symmetrically laminated composite plates with first-order shear deformation theory (fsdt) by discrete singular convolution method. Finite Elements in Analysis and Design, 44:725–731, 2008.
28. R.W. Clough and J.I. Tocher. Finite element stiffness matrix for the analysis for plate bending. Proc. Conf. Matrix Meth. Struct. mech., pages 515–546, 1965.
29. R.R. Craig. Coupling of substructures for dynamic analysis: an overview. AIAA Journal, 1573, 2000.
30. R.R. Craig and M.C.C. Bampton. Coupling of substructures for dynamic analysis. AIAA Journal, 6(7):1313–1319, 1968.
31. S. de Miranda and F. Ubertini. A simple hybrid stress element for shear deformable plates. International Journal For Numerical Methods in Engineering, 65:808–833, 2006.
32. M. Duan, Y. Miyamoto, S. Iwasaki, and H. Deto. Numerical implementation of hybrid-mixed finite element model for reissner-mindlin plates. Finite Element in Analysis and Design, 33:167–185, 1999.
33. N. Fantuzzi and F. Tornabene. Strong formulation finite element method for arbitrarily shaped laminated plates - part 1. theoretical analysis. Advances in Aircraft and Spacecraft Science, 1:125–143, 2014.
34. N. Fantuzzi and F. Tornabene. Strong formulation finite element method for arbitrarily shaped laminated plates - part 2. numerical analysis. Advances in Aircraft and Spacecraft Science, 1:145–175, 2014.
35. N. Fantuzzi, F. Tornabene, E. Viola, and A.J.M. Ferreira. A strong formulation finite element method (sfem) based on rbf and gdq techniques for the static and dynamic analyses of laminated plates of arbitrary shape. Meccanica, 49:2503–2542, 2014.
36. A.J.M Ferreira, L.M.S Castro, and S Bertoluzza. Analysis of plates on winkler foundation by wavelet collocation. Meccanica, 46:865–873, 2011.
37. B. Fraeijs de Veubeke. Displacement and equilibrium models in the finite element method, chapter 9. John Wiley & Sons, 1965.
38. B. Fraeijs de Veubeke and G. Sander. An equilibrium model for plate bending. International Journal of Solids and Structures, 4:447–768, 1968.
39. R. Garcia Lage, C.M. Mota Soares, C.A. Mota Soares, and J.N. Reddy. Analysis of adaptative plate structures by mixed layerwise finite elements. Composite and Structures, 66:269–276, 2004.
40. R. Garcia Lage, C.M. Mota Soares, C.A. Mota Soares, and J.N. Reddy. Modelling of piezolaminated plates using layerwise mixed elements. Computers and Structures, 82:1849–1863, 2004.
41. M. Gellert and M.E. Laursen. Formulation and convergence of a mixed finite element method applied to elastic arches of arbitrary geometry and loading. Computer Methods In Applied Mechanics and Engineering, 7:285–302, 1976.
42. E. Hellinger. Die allgemeinen ansatze der mechanik der kontinua. Encyklopadie der mathematischen Wissenschaften, 4, 1914.
43. R.D. Henshell. A theoretical basis for hybrid finite elements in dynamic problems. Journal of Sound and Vibration, 39 (4):520–522, 1975.
44. R.D. Henshell, D. Walters, and G.B. Warburton. A new family of curvilinear plate bending elements for vibration and stability. Journal of Sound and Vibration, 20 (3):381–397, 1972.
45. L.R. Herrmann. A bending analysis for plates. Proceeding of the conference on matrix methods in structural mechanics, A.F.F.D.L-TR-66-88, pages 577–604, 1965.
46. L.R. Herrmann. Finite element bending analysis. Journal of the Engineering Mechanics Division, A.S.C.E EM5, 93:13–26, 1967.
47. T.J.R. Hughes, M. Cohen, and M. Haron. Reduced and selective integration techniques in the finite element analysis of plates. Nuclear Engineering and Design, 46:203–222, 1978.
48. L. Jézéquel and H.D. Setio. Component modal synthesis methods based on hybrid models, part 1: Theory of hybrid models and modal truncation methods. Journal of Applied mechanics, 61:100–108, 1994.

49. L. Jézéquel and H.D. Setio. Component modal synthesis methods based on hybrid models, part 2: numerical test analyses experimental identification of hybrid models. Journal of Applied Mechanics, 61(1):109–116, 1994.
50. F. Koschnick, M. Bischoff, N. Camprubì, and K.U. Bletzinger. The discrete strain gap method and membrane locking. Computer Methods in Applied Mechanics and Engineering, 194:2444–2463, 2005.
51. S.W. Lee and J.J. Rhiu. A new efficient approach to the formulation of mixed finite element model for structural analysis. International Journal For Numerical Methods In Engineering, 21:1629–1641, 1986.
52. K.M. Liew and J.-B Han. A four-node differential quadrature method for straight-sided quadrilateral reissner/mindlin plates. Communications in Numerical Methods in Engineering, 13:73–81, 1997.
53. K.H. Lo, R.M. Christensen, and M. Wu. A high-order theory of plate deformation—part 2: Laminated plates. Journal of Applied Mechanics, 44:669–676, 1977.
54. A.E.H. Love. On the small free vibrations and deformations of elastic shells. Philosophical Transactions of the Royal Society of London, 17:491–549, 1888.
55. R.H. MacNeal. A hybrid method of component mode synthesis. Computers and Structures, 1:581–601, 1971.
56. R.D. Mindlin. Influence of rotatory inertia and shear on flexural motions of isotropic, elastic plates. Journal of Applied Mechanics, 18:31–38, 1951.
57. H. Nguyen-Xuan, G.R. Liu, C. Thai-Hoang, and T. Nguyen-Thoi. An edge-based smoothed finite element method (es-fem) with stabilized discrete shear gap technique for analysis of reissner-mindlin plates. Computational Methods Applied for Mechanical Engineering, 199:471–489, 2010.
58. M.H. Omurtag and F. Kadioglu. Free vibration analysis of orthotropic plates resting on pasternak foundation by mixed finite element formulation. Computers and Structures, 67:253–265, 1998.
59. T.H.H. Pian, D.P. Chen, and D. Kang. A new formulation of hybrid/mixed finite element. Computers & Structures, 16:81–87, 1983.
60. T.H.H. Pian and P. Tong. Finite element methods in continuum mechanics. Advances in Applied Mechanics, 12:1–58, 1972.
61. G. Prange. Die variations- und minimalprinzipie der statik der baukonstruktion (doctoral dissertation). Habilitationsschrift, Technische Hochschule Hannover, 1916.
62. J.N. Reddy. A generalization of two-dimensional theories of laminated composite plates. Communications in Applied Numerical Methods, 3:173–180, 1987.
63. J.N. Reddy. Theory and Analysis of Elastic Plates and Shells. 2007.
64. E. Reissner. The effect of transverse shear deformation on the bending of elastic plates. Journal of Applied Mechanics, 12:69–76, 1945.
65. E. Reissner. On a variational theorem in elasticity. Journal of Mathematics and Physics, 29:90–95, 1950.
66. E. Reissner. On a certain mixed variational theorem and a proposed application. International Journal For Numerical Methods In Engineering, 20(7):1366–1368, 1984.
67. E. Reissner. On a mixed variational theorem and on shear deformable plate theory. International Journal For Numerical Methods In Engineering, 23(2):193–198, 1986.
68. A.F. Saleeb and T.Y. Chang. On the hybrid-mixed formulation of c0 curved beams. Computer Methods in Applied Mechanics and Engineering, 60:95–121, 1987.
69. N. Srinivas. A refined analysis of composite laminates. Journal of Sound and Vibration, 30(4):495–507, 1973.
70. H. Stolarski and T. Belytschko. Shear and membrane locking in curved c0 elements. Computer methods in applied mechanics and engineering, 41:279–296, 1983.
71. H. Stolarski and T. Belytschko. On the equivalence of mode decomposition and mixed finite element based on the hellinger-reissner principle. part 1: Theory. Computers Methods in Applied Mechanics and Engineering, 58:249–263, 1986.
72. H. Stolarski and T. Belytschko. On the equivalence of mode decomposition and mixed finite element based on the hellinger-reissner principle. part 2: Application. Computers Methods in Applied Mechanics and Engineering, 58:265–284, 1986.
73. P. Tong and T.H.H. Pian. A variational principle and the convergence of a finite element method based on assumed stress distribution. International Journal of Solids and Structures, 5:463–472, 1969.
74. F. Tornabene, N. Fantuzzi, E. Viola, and R.C. Batra. Stress and strains recovery for functionally graded free-form and doubly-curved sandwich shells using higher-order equivalent single layer theory. Composite and Structures, 119:67–89, 2015.
75. F. Tornabene, N. Fantuzzi, E. Viola, M. Cinefra, E. Carrera, A. Ferreira, and A.M. Zenkour. Analysis of thick isotropic and cross-ply laminated plates by generalized differential quadrature method and a unified formulation. Composites. Part B, Engineering, 58:544–552, 2014.
76. D.M. Tran. Component mode synthesis methods using interface modes. application to structures with cyclic symmetry. Computers and Structures, 79:209–222, 2001.

-
77. K. Washizu. Variational methods in elasticity and plasticity, 2nd edition. Pergamon Press, 1975.
 78. P. Wriggers and C. Carstensen. Mixed Finite Element Technologies. Applied Mathematics/Computational Methods of Engineering, 2009.
 79. F. Wu, G.R. Liu, G.Y. Li, A.G. Cheng, and Z.C. He. A new hybrid-smoothed fem for static and free vibration analyses of reissner-mindlin plates. Computational Mechanics, 54(3):865–890, 2014.
 80. S Xiang, H Shi, K.M Wang, Y.T Ai, and Y.D Sha. Thin plate spline radial basis functions for vibration analysis of clamped laminated composite plates. European Journal of Mechanics - A/Solids, 29:844–850, 2010.
 81. O.C. Zienkiewicz and Y.K. Cheung. The finite element method in structural and continuum mechanics. McGraw-Hill, 1967.